Carbohydrate Research 345 (2010) 141–147

Contents lists available at ScienceDirect

Carbohydrate Research

journal homepage: www.elsevier.com/locate/carres

Solid-state structures and thermal properties of inclusion complexes of the organophosphate insecticide fenitrothion with permethylated cyclodextrins

Dyanne Cruickshank [a], Natalia M. Rougier [b], Raquel V. Vico [b], Rita H. de Rossi [b], Elba I. Buján [b], Susan A. Bourne [a], Mino R. Caira [a,*]

[a] Department of Chemistry, University of Cape Town, Rondebosch 7701, South Africa
[b] Instituto de Investigaciones en Físico Química de Córdoba (INFIQC), Departamento de Química Orgánica, Facultad de Ciencias Químicas, Universidad Nacional de Córdoba, Ciudad Universitaria, X5000HUA Córdoba, Argentina

ARTICLE INFO

Article history:
Received 11 September 2009
Received in revised form 19 October 2009
Accepted 28 October 2009
Available online 3 November 2009

Keywords:
Fenitrothion
Permethylated cyclodextrins
Single crystal X-ray diffraction
Thermal analysis
Inclusion complexes

ABSTRACT

The X-ray crystal structures and thermal stabilities of the inclusion complexes formed between the organophosphate insecticide fenitrothion [*O*,*O*-dimethyl *O*-(3-methyl-4-nitrophenyl) phosphorothioate] and the host compounds TRIMEA and TRIMEB (permethylated α- and β-cyclodextrins, respectively) are reported. In the complex (TRIMEA)$_2$·fenitrothion **1**, the guest phosphate ester group is disordered and the molecule is fully encapsulated within a novel TRIMEA dimer in which the secondary rims of the two host molecules are in close contact. In contrast, the complex TRIMEB·fenitrothion **2** is monomeric and the guest molecule is statistically disordered over two positions, with the phosphate group inserted in the host cavity in both cases. Thermal analysis indicated gradual and partial loss of the guest in **1** during heating between 130 °C and the melting point of the complex (~200 °C), whereas complex **2** displayed significant mass loss only after fusion of the complex at 161 °C.

© 2009 Elsevier Ltd. All rights reserved.

1. Introduction

Molecular encapsulation of organophosphate pesticides by cyclodextrins (CDs) can enhance the efficacy and facilitate formulation of these agrochemicals in a variety of ways, for example, by increasing their flowability, wettability, dissolution rate, chemical and thermal stability, and reducing their volatility.[1] The interaction between CDs and the widely used broad spectrum insecticide and acaricide, fenitrothion [*O*,*O*-dimethyl *O*-(3-methyl-4-nitrophenyl) phosphorothioate, Fig. 1], has been investigated in several contexts. These include studies of the inhibition of the hydrolytic degradation of fenitrothion by native CDs,[2,3] the formulation of fenitrothion as a CD complex containing also a bioactive synergist to enhance insecticidal activity,[4,5] and the development of insecticidal construction materials based on fenitrothion–CD inclusion complexes.[6]

Knowledge of the probable mode of guest inclusion within a CD is necessary for a mechanistic interpretation of catalytic effects, such as the solution-phase CD-inhibited hydrolysis of fenitrothion,[3] or the enhancement, or otherwise, of the thermal stability of guest compounds through the formation of their solid CD inclusion complexes.[7] In the former case, kinetics studies coupled with theoretical calculations indicate that the fenitrothion molecule is protected from nucleophilic attack by deep insertion of the phosphate group within the β-CD cavity.[3] On the other hand, the lack of published data on the mode of fenitrothion inclusion in CDs in the solid state hinders the interpretation of analogous processes that its crystalline inclusion complexes may undergo.

In this report, we describe the modes of inclusion of fenitrothion in its inclusion complexes with two derivatised CDs, namely hexakis(2,3,6-tri-*O*-methyl)-α-CD (TRIMEA) and heptakis(2,3,6-tri-*O*-methyl)-β-CD (TRIMEB), as determined by single crystal X-ray diffraction. Novel structural results, of interest from both the agrochemical and CD crystal packing viewpoints, are presented. These structures are also briefly discussed in the context of the observed thermal behaviour of the inclusion complexes.

In contrast to the organophosphate pesticide analogues iodofenphos, methylparathion, famphur and ronnel, for which room-tem-

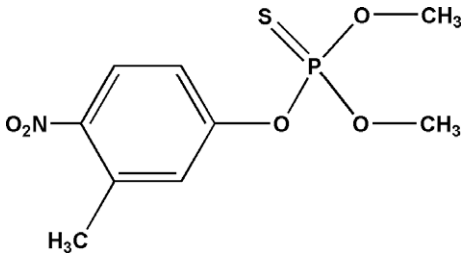

Figure 1. Chemical structure of the organophosphate insecticide fenitrothion.

* Corresponding author.
E-mail address: Mino.Caira@uct.ac.za (M.R. Caira).

0008-6215/$ - see front matter © 2009 Elsevier Ltd. All rights reserved.
doi:10.1016/j.carres.2009.10.023

perature X-ray structures have been reported,[8] fenitrothion is an oil at an ambient temperature and its structure in the solid state has not been reported to date. Thus, the X-ray structures of the inclusion complexes of fenitrothion presented here yield the first accurate molecular parameters for the insecticide molecule as well as indications of possible conformations that it may adopt. Since fenitrothion is thermolabile,[9] NMR spectroscopy of dissolved inclusion complex crystals was employed in this study to confirm the structural integrity of fenitrothion following complex preparation by co-precipitation from aqueous solution at elevated temperatures.

2. Experimental

2.1. Materials and solid complex preparation

The host compounds hexakis(2,3,6-tri-*O*-methyl)-α-CD (TRIMEA) and heptakis(2,3,6-tri-*O*-methyl)-β-CD (TRIMEB) were purchased from Cyclolab (Budapest, Hungary) and were used as received. Fenitrothion was isolated as a yellow oil from a commercial sample of Sumithion (Sumitomo Chemical, NY, USA) by column chromatography over silica gel and was characterized by ^{1}H and ^{31}P NMR spectroscopy and GC–MS. For complex preparation by the co-precipitation method, distilled water was used. Solvents for NMR spectroscopy included D_2O (deuterium content 99.9%), obtained from Merck (Germany) as well as $CDCl_3$ and DMSO-d_6 (Sigma–Aldrich, USA).

The inclusion complex between TRIMEA and fenitrothion was prepared by adding an equimolar amount of the guest to a saturated aqueous solution of TRIMEA at 20 °C. Stirring for several hours and subsequent heating to 60 °C led to a turbid solution which was then removed from the hot plate and stirred at room temperature. This process was repeated until a clear solution was obtained at room temperature. Following filtration through a 0.45 μm microfilter, the clear solution was placed in an oven at 60 °C. Colourless single crystals of the inclusion complex **1** formed over a 12 h period.

A similar procedure was used to prepare the inclusion complex **2** between TRIMEB and fenitrothion. The preparation commenced with a saturated solution of TRIMEB at 40 °C, to which an equimolar amount of fenitrothion was added. Continuous stirring and cycling through heating and cooling cycles (as for the preparation of complex **1**) yielded a clear solution that was filtered and placed in a Dewar flask containing water at 60 °C. After five days, a powder had formed. Upon standing at room temperature for one month, colourless single crystals of **2** appeared.

2.2. Thermal analysis

Thermogravimetric analysis (TGA) and differential scanning calorimetric (DSC) measurements were performed using a Mettler Toledo TGA analyser and a Perkin–Elmer DSC7 instrument with dry nitrogen purge gas flowing at 30 cm^3 min^{-1} in each case. Samples in the range 2–4 mg were surface-dried on a filter paper, accurately weighed, placed in alumina crucibles and vented platinum pans for the respective analyses and heated at a constant rate of 10 K min^{-1} in the range 30–300 °C. For hot stage microscopy (HSM), samples were placed under silicone oil on a cover slip and viewed with a Nikon SMZ-10 stereomicroscope fitted with a Linkam THM hot stage and a Linkam TP92 temperature control unit.

2.3. ^{1}H and ^{31}P NMR spectroscopy

NMR spectroscopy was employed to determine inclusion complex stoichiometry and to monitor the integrity of the thermolabile guest fenitrothion. Samples of the inclusion complex crystals were prepared in $CDCl_3$, D_2O and DMSO-d_6. ^{1}H and ^{31}P NMR spectra were recorded at 300 MHz on a Varian Gemini 300 spectrometer at 298 K.

2.4. Single crystal X-ray diffraction

Intensity data collection for the complex (TRIMEA)$_2$·fenitrothion **1** was performed on a Bruker KAPPA APEX II DUO diffractometer. For TRIMEB·fenitrothion **2**, intensity data were measured on a Nonius Kappa CCD diffractometer. Both crystals were maintained at 173(2) K using Cryostream coolers (Oxford Cryosystems UK). For complex **1**, unit cell refinement and data reduction were performed using the program SAINT.[10] The programs DENZO-SMN and SCALEPACK were used for unit cell refinement and data reduction for **2**.[11] For both **1** and **2**, the Laue system was found to be *mmm*, indicating the orthorhombic crystal system and the common space group $P2_12_12_1$ was uniquely identified from systematic absences. Data were corrected for Lorentz-polarization effects and for absorption (program SADABS[12]). Structure solution for **1** was achieved by direct methods (program SHELXD[13]) while the phase problem for complex **2** was solved by using the host atomic coordinates of the isostructural complex TRIMEB·(*S*)-naproxen[14] as a trial model. All non-hydrogen atoms except O6, C7, C8 and C9 of each methyl glucose unit were included in the fragment serving as the trial model.

Structure development and least-squares refinement for **1** and **2** were not routine and further details follow. Examination of the two crystallographically independent TRIMEA molecules (A, B) in **1** revealed twofold disorder of three methoxy groups, namely one secondary –OCH_3 group on glucose residue B5 and the primary –OCH_3 groups on residues B2 and B5. Disorder was modelled by allowing the two components to refine isotropically with site-occupancy factors (s.o.f.s) x and $1 - x$. All host atoms except those of the disordered components and six ordered atoms were treated anisotropically in full-matrix least-squares refinement (program SHELXH-97[15]). Attempted refinement of the six ordered atoms produced unrealistic ellipsoids due to their high thermal motion. The single guest molecule in the asymmetric unit was located by difference Fourier (ΔF) techniques. Initially, all atoms expected for the fenitrothion molecule, except those of the *O*,*O*-dimethyl phosphorothioate unit, were clearly discernible and refined very satisfactorily. The appearance of more than the expected number of ΔF peaks around the phosphorus atom suggested either molecular disorder or possible decomposition of the fenitrothion molecule (fenitrooxon, the *S*-methyl isomer of fenitrothion, and 3-methyl-4-nitrophenol being known decomposition products).[9] At this point, employment of ^{31}P NMR spectra of the crystal batch (see Section 3.1 below) gave unequivocal proof that the included fenitrothion molecule was intact. Subsequent refinement and careful examination of ΔF maps revealed twofold disorder of both the sulfur atom and one of the –OCH_3 groups. All guest atoms, except those attached to the phosphorus atom, were refined anisotropically, with appropriate distance constraints (four O–C and two P–O bonds) applied to the disordered moieties. Owing to the high resolution of the X-ray data, some of the guest H atoms were also apparent in ΔF maps. However, all H atoms were finally added in idealised positions in a riding model with U_{iso} 1.2–1.5 times those of their parent atoms. The s.o.f.s of the major and minor components of guest disorder refined to 0.57 and 0.43, respectively.

The asymmetric unit in complex **2** comprises one TRIMEB molecule and one guest molecule. Refinement of the host molecule revealed twofold disorder of the primary methoxy group on glucose residue G6. This was modelled as for complex **1**. Anisotropic refinement followed for all ordered atoms except for C9G3 (U_{iso} ~0.12 Å^2), for which an unacceptable ellipsoid was produced on attempted anisotropic refinement due to its relatively high thermal

motion. Twofold disorder of the included fenitrothion molecule, with no shared atoms, was evident from ΔF maps. This was similarly modelled by assigning global s.o.f.s of x and $1 - x$ to the two disordered components, the value of x refining to 0.66. Several distance constraints were applied to maintain reasonable guest geometry. Guest atoms were refined with individual isotropic thermal parameters. The same H atom treatment described for complex **1** was applied to complex **2**.

3. Results and discussion

3.1. Preliminary complex characterization

Since crystallization of methylated CD inclusion complexes is usually carried out at elevated temperature,[16] sensitive guest compounds may undergo chemical modification during complex preparation. The known thermolabile nature of fenitrothion and its analogues[9,17,18] prompted the use of ^{31}P NMR spectroscopy as a tool for confirming the presence of the intact molecule in complex **1**, for which initial X-ray diffraction results indicated either molecular disorder in the phosphorothioate moiety or potential guest decomposition, as outlined in Section 2.4 above. Previous work indicated that fenitrothion is readily distinguished from its thermal decomposition product, mainly the *S*-methyl isomer, *O*,*S*-dimethyl [*O*-(4-nitro-*m*-tolyl)] phosphorothioate, from ^{31}P chemical shifts.[9,19] In the present study, ^{31}P proton-decoupled NMR spectra for a freshly prepared sample of fenitrothion and a solution of crystalline complex **1** in the common solvent $CDCl_3$ were recorded, yielding in each case a single peak at $\delta = 65.456$ and 65.459 ppm, respectively, in accord with the data obtained previously for fenitrothion.[20] The host–guest stoichiometry of 2:1 for **1** was established from ^{1}H NMR integration while elemental analysis confirmed the 1:1 stoichiometry for **2** (Anal. Calcd for $C_{63}H_{112}O_{35}{\cdot}C_9H_{12}O_5NPS$: C, 50.67; H, 7.32; N, 0.82. Found: C, 50.60, H, 7.43, N, 0.61).

Table 1
Crystal data and structure refinement for the complexes **1**and **2**

	1	**2**
Chemical formula	$(C_{54}H_{96}O_{30})_2{\cdot}C_9H_{12}O_5NPS$	$C_{63}H_{112}O_{35}{\cdot}C_9H_{12}O_5NPS$
Formula weight	2727.84	1706.75
Crystal system	Orthorhombic	Orthorhombic
Unit cell constants		
Space group	$P2_12_12_1$	$P2_12_12_1$
a (Å)	15.097(2)	15.1588(4)
b (Å)	24.278(3)	21.1279(4)
c (Å)	38.385(4)	27.5575(7)
$\alpha = \beta = \gamma$ (°)	90	90
V (Å^3)/Z	14,069(3)/4	8825.9(4)/4
D_{calcd} (g cm^{-3})	1.288	1.284
Temperature (K)	173(2)	173(2)
Wavelength (Å)	0.71073	0.71073
Dimensions (mm)	0.11 × 0.04 × 0.03	0.24 × 0.13 × 0.11
θ-Range collection (°)	1.91–25.09	2.69–25.70
Index range	$-18 \leqslant h \leqslant 6$ $-27 \leqslant h \leqslant 28$ $-45 \leqslant h \leqslant 34$	$-18 \leqslant h \leqslant 18$ $-25 \leqslant h \leqslant 25$ $-33 \leqslant h \leqslant 33$
Reflections collected	47,709	121,751
Independent reflections	24,600	16,732
Reflections with $[I > 2\sigma(I)]$	14,645	11,175
Number of parameters	1661	959
R_{int}	0.0462	0.0568
Goodness of fit	1.010	1.021
R_1 $[I > 2\sigma(I)]$	0.0638	0.0626
wR_2	0.1401	0.1428
Largest difference peak and hole (e Å^{-3})	0.61/−0.39	0.71/−0.74

3.2. Single crystal X-ray structures

Table 1 lists crystal data and refinement details for the complexes **1** and **2**. Inclusion complexes of TRIMEA are generally monomeric.[8] Complex **1** (Fig. 2) is the first example of a TRIMEA inclusion complex in which a guest molecule is encapsulated within a host head-to-head dimer. [In the inclusion complex $(TRIMEA)_2$·metoprolol, the only other known dimeric TRIMEA complex, whose structure we reported recently,[21] the guest is contained within a cage formed by head-to-tail contact of two TRIMEA molecules]. Host molecule A accommodates the aromatic portion of the fenitrothion molecule while the *O*,*O*-dimethyl phosphorothioate unit is contained within the cavity of host molecule B (Fig. 2, top). The host molecules are laterally offset from each other for optimal guest encapsulation (Fig. 2, bottom). Several primary methoxy groups on hosts A and B act as 'lids', sealing the capsule at both ends.

From the geometric parameters for the crystallographically non-equivalent host molecules A and B listed in Table 2, it is evident that host molecule A is considerably more distorted than molecule B. The former adopts an elliptical shape to accommodate the planar methyl-nitrophenyl moiety, while the latter, containing the more isotropic *O*,*O*-dimethyl phosphorothioate unit, adopts a more 'round' shape. Figure 3 shows perspective views of host molecules A and B, containing, respectively, the aromatic and dimethyl phosphorothioate groups, viewed from within the cavity, that is, from their secondary rims. The ellipticity of the O4-hexagon in molecule A is evident from the wide range of radii values (l, Table 2), namely 3.79–4.58 Å. The transannular distance O4A3···O4A6 (Fig. 3), normal to the plane of the included aromatic ring, is only 7.61 Å, whereas O4A1···O4A4, which is roughly parallel to the included ring plane, is 8.95 Å. Instead, for host B, the values of l span the narrow range 4.10–4.41 Å. The more severe distortion of host A is also reflected in wider ranges of the parameters D and ϕ when

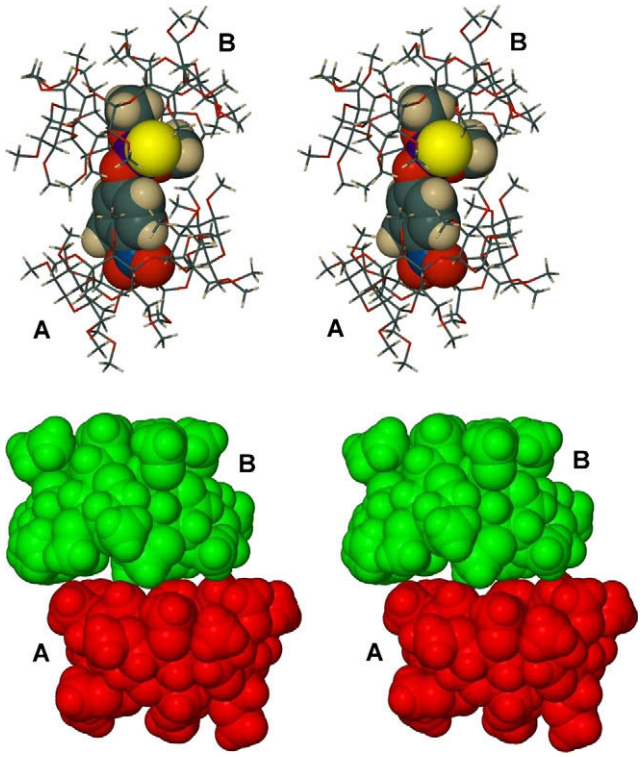

Figure 2. Stereoviews of the 2:1 host–guest unit in complex **1** with only the major disordered guest component shown (top) and a space-filling diagram of the TRIMEA dimer (bottom).

Table 2
Geometrical parameters for the host molecules in complexes **1** and **2**

Residue	l[a] (Å)	D[b] (Å)	ϕ[c] (°)	d[d] (°)	α[e] (Å)	D_3[f] (Å)	τ[g] (°)
Complex **1**							
A1	4.52	4.05	113.1	−13.5	0.231	3.321	28.7
A2	4.50	4.39	113.9	9.5	−0.259	3.347	24.1
A3	3.82	4.44	130.8	5.6	0.035	3.590	6.8
A4	4.45	3.95	116.4	−12.0	0.219	3.369	32.2
A5	4.58	4.55	111.0	7.4	−0.239	3.301	20.2
A6	3.79	4.38	132.5	7.1	0.013	3.699	14.3
B1	4.41	4.12	114.4	−3.4	−0.084	3.306	−3.4
B2	4.10	4.47	126.5	−0.8	0.005	3.800	38.7
B3	4.40	4.15	114.8	2.3	0.058	3.561	7.2
B4	4.26	4.42	122.6	0.6	−0.043	3.683	30.7
B5	4.31	4.19	117.3	−5.4	−0.041	3.237	9.8
B6	4.18	4.33	124.2	6.6	0.105	3.450	27.8
Complex **2**							
G1	5.18	4.49	124.5	5.7	0.239	3.404	16.4
G2	4.89	4.26	129.2	−23.5	0.441	3.088	28.0
G3	4.83	4.41	131.3	0.8	−0.384	3.242	35.2
G4	5.14	4.40	124.4	25.5	−0.340	3.569	−15.3
G5	5.15	4.29	120.7	−19.0	0.603	3.831	36.5
G6	4.65	4.47	138.2	−12.1	−0.017	3.341	44.2
G7	5.11	4.28	122.6	19.2	−0.541	3.459	−12.1

[a] Radius O(4n)···(centroid of the O4 atoms).
[b] Glycosidic O4n···O4(n + 1) distance.
[c] O4(n − 1)···O4n···O4(n + 1) angle.
[d] O4(n − 1)···O4n···O4(n + 1)···O4(n + 2) torsion angle.
[e] Deviation of atoms O4n from the least-squares planes (mean e.s.d. 0.002 Å).
[f] Inter-ring O2(n)···O3(n − 1) distance (mean e.s.d. 0.006 Å).
[g] Tilt angle between the O(4) plane and the mean plane through the atoms O4(n)···C(4n)···C(1n)···O4(n − 1) (mean e.s.d. 0.1°).

compared with the data obtained for host B, larger magnitudes in torsion angles (d) and more significant deviations from the O4-plane (α) (Table 2). In accommodating the phosphate ester residue, host B maintains a 'round' shape (based on the uniform radii l), though the individual glucose rings tilt (as reflected in the parameter τ) with a range of angles wider than those for host A.

The nature of the guest disorder in complex **1** is shown in Figure 4, where for clarity the entire molecules (a, b) are drawn for what are essentially two rotamers, the *O*,*O*-dimethyl phosphorothioate groups being rotated by 107° with respect to one another around the O11–P12 bond. The two components (a, b) thus share all atoms except the sulfur atom and one of the –OCH_3 groups. The major rotamer (a), containing S15A and the methoxy group –O16A–C17A, has a refined s.o.f. of 0.57 while its counterpart has s.o.f. 0.43. Conformational differences are reflected in a range of S=P–O–C torsion angles. The unrestrained P=S bond lengths refined to 1.894(5) and 1.906(8) Å, respectively. Major conformational features include the slight twist of the nitro group out of the plane of the aromatic ring (the dihedral angle C4–C3–N8–O9 is −16.3(7)°) and the *gauche* conformation around the bond C6–O11 linking the aromatic moiety to the dimethyl phosphorothioate group (C5–C6–O11–P12 = 57.9(8)°). A search for hydrogen bonds between host and guest revealed only two significant interactions, namely C7–H···O2B3, linking a phenyl hydrogen atom to a host methoxy oxygen atom (H···O 2.38 Å, C···O 3.309(6) Å and angle C–H···O 167°), and C5A6–H···O10 (H···O 2.53 Å, C···O 3.482(6) Å and angle C–H···O 159°), linking a methine H atom to an oxygen atom of the nitro group.

Packing of the 2:1 host–guest complex units is of the 'cage' variety (Fig. 5), the primary ends of each dimeric unit being abutted by side-on contact with host molecules of complex units related by the twofold screw axis parallel to *c*. Fenitrothion molecules are isolated from one another by complete encapsulation within the dimers. Cohesion between host molecules is maintained by several C–H···O hydrogen bonds. TRIMEA inclusion complexes are

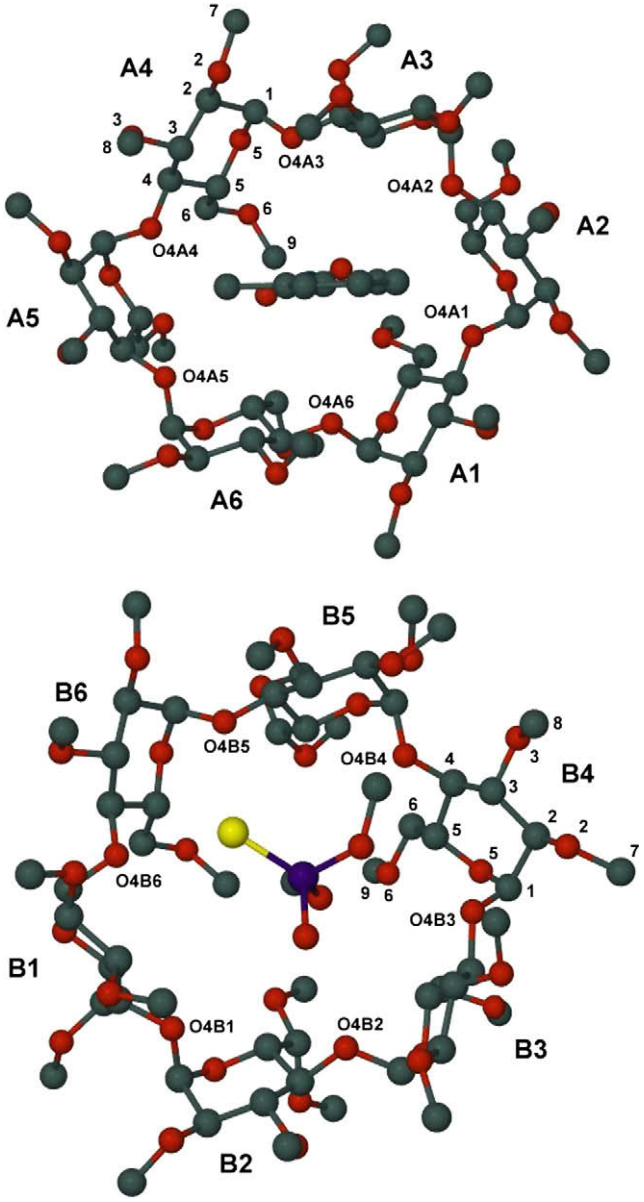

Figure 3. Host molecules A and B in complex **1** with atom and glucose residue labelling, viewed from their secondary sides and including their respective guest moieties.

generally monomeric with 1:1 host–guest stoichiometry, the majority crystallizing in head-to-tail channel-mode in the space group $P2_1$.[8] The only other known dimeric complex, mentioned above, has 2:1 stoichiometry and a head-to tail dimer, with identical packing to that of the monomeric complexes.[21] Thus, the complex **1** is unique with respect to both the nature of the dimer and the crystal packing.

The monomeric complex unit of **2** is shown in Figure 6. For clarity, only the major component of twofold guest disorder (with s.o.f. 0.66) is shown in the cavity of the host TRIMEB. The guest *O*,*O*-dimethyl phosphorothioate residue is deeply embedded, in contact with the 'roof' of the host cavity, formed by the primary methoxy groups of glucose residues G1, G2, G3 and G6. A space-filling representation shows that virtually the entire molecule is included within the host cavity, only the nitro group protruding from the secondary side. The host geometrical parameters (Table 2) are very similar to those reported for the isostructural complex TRIMEB·(*S*)-naproxen.[14]

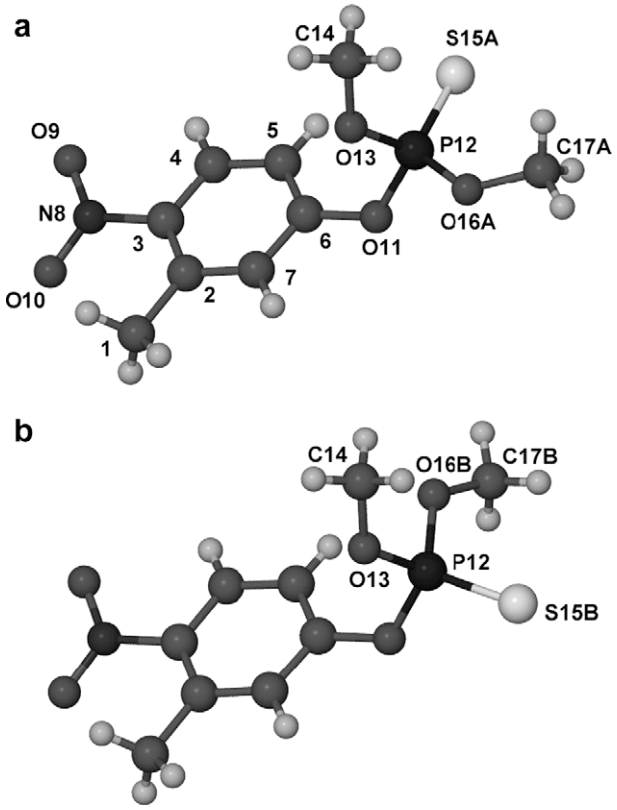

Figure 4. Rotamers of fenitrothion giving rise to twofold disorder in complex **1**.

In contrast to the situation in complex **1**, the disordered guest model in **2** comprises two distinct molecules of fenitrothion (Fig. 7), the component containing the phosphorus atom labelled A being the major component (s.o.f. 0.66). The methyl nitrophenyl ring planes are related by an approximate twofold rotation axis as well as a lateral shift. (In fact, the aromatic ring planes are not coplanar but intersect at ~15°.) Furthermore, as found for the fenitrothion molecule in complex **1**, the disordered components in **2** are distinct rotamers which include in the TRIMEB cavity in a similar fashion. No significant hydrogen bonds occur between the host and guest molecules.

Crystal packing for complex **2** is shown in Figure 8. Monomeric units of TRIMEB·fenitrothion pack in screw-channel mode in a head-to-tail fashion. In this well-known packing arrangement, alternate host molecules in a particular column parallel to the *b*-axis are offset by several Ångstroms in the *x*-direction, resulting in an undulating host channel, as opposed to a linear one. This packing arrangement differs from that found in monoclinic TRIMEB complexes [e.g., with guests butamben, EZAVOQ and 2,4-dichlorophenoxyacetic acid, ASIQOI][8] where the channel is linear. The nitro group occupies an interstitial void created by surrounding host molecules. Several C–H···O hydrogen bonds linking host molecules were identified. The principal ones are C14A–H···O4G6 (H···O 2.70 Å, C···O 3.483(5) Å, C–H···O 136°), C14A–H···O2G7 (H···O 2.70 Å, C···O 3.438(5) Å, C–H···O 131°) and C14B–H···O6G6 (H···O 2.49 Å, C···O 3.182(5) Å, C–H···O 128°).

While inclusion complexes of methylated CDs may contain a small percentage of water of crystallization, both **1** and **2** are anhydrous, though crystallized from aqueous media. Thus, close packing of complex units is achieved without incorporation of water molecules into the crystals.

3.3. Thermal analysis

The thermal stability of a compound may differ depending on whether it is examined as a pure material, in solution or in the form of an inclusion compound. In particular, the boiling point of a pure liquid may be significantly less than or greater than its temperature of desolvation from an inclusion crystal, depending on the topology of guest inclusion (viz. channel-mode vs isolated-site occupation).[22]

In a study of the thermal decomposition of pure fenitrothion, Tsuji et al. reported that DTA analysis under nitrogen yields two exothermic peaks in the ranges 210–235 °C and 270–285 °C, and they identified possible decomposition products.[17] As part of the characterization of inclusion complexes **1** and **2**, it was of interest to record their behaviour on heating to establish whether the thermal stability of fenitrothion in these forms differs materially from that of pure fenitrothion. Combined TGA, DSC and HSM results are shown in Figures 9 and 10, respectively.

For the TRIMEA complex **1**, the TG profile (Fig. 9) under nitrogen indicates an initial linear mass loss of ~7% commencing at around 130 °C, interpreted as gradual loss of fenitrothion from the inclusion complex (total theoretical mass loss for the 2:1 inclusion complex: 10.2%). This is accompanied by the broad

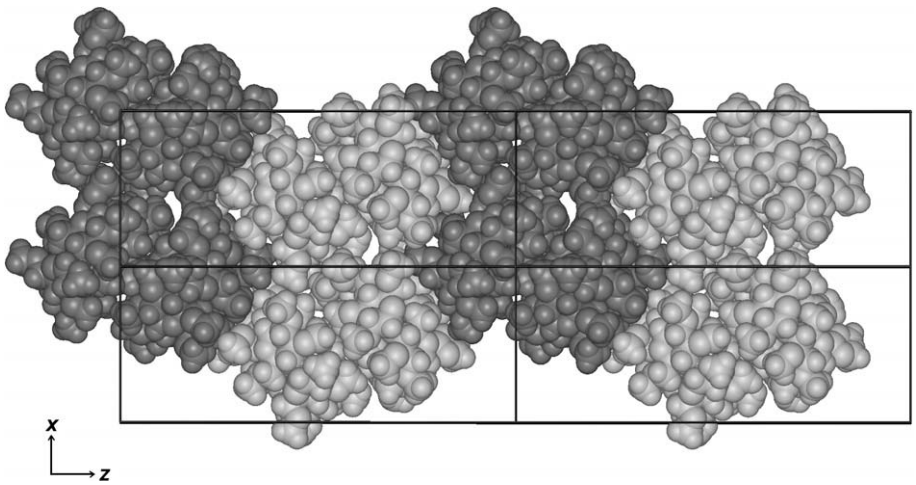

Figure 5. Space-filling representation of the cage-type packing of complex **1**. Four unit cells are shown and the screw-related dimeric complex units are distinguished by their shading.

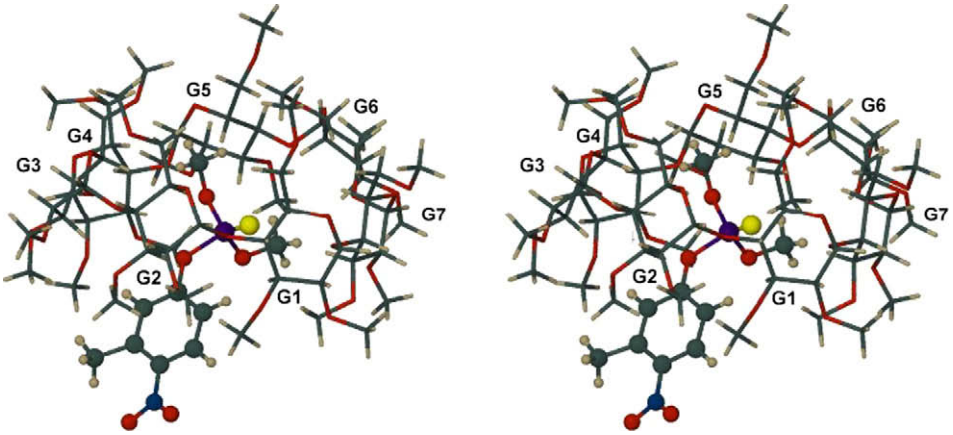

Figure 6. Stereoview of the complex **2** with host residue numbering. For clarity, only the major component of guest disorder is included in the host.

endothermic peak at ~135 °C in DSC as well as crystal cracking, with evidence of bubble evolution in HSM. The second endotherm peaking at ~205 °C corresponds to the fusion of the host TRIMEA, which subsequently decomposes, possibly with simultaneous decomposition of the released guest. It seems reasonable to conclude that prior to fusion of the host, the absence of exothermic effects implies that fenitrothion does not decompose. From the results of single crystal X-ray diffraction, which indicated virtually complete encapsulation of the fenitrothion molecule within the TRIMEA dimer, it is difficult to rationalise the escape of the guest from the crystal. A reasonable assumption is that thermal agitation during heat absorption in the region of 130 °C causes a rearrangement of the solid complex to a structure conducive to guest escape. Thereafter, the remaining TRIMEA would decompose endothermically at the expected temperature, as observed.

Analogous thermal data for the TRIMEB complex are shown in Figure 10. The only significant feature in the DSC trace is the endotherm peaking at ~161 °C (d) and there was no appreciable TG mass loss prior to this temperature. The thermal profiles are simpler than those for complex **1** and indicate that the inclusion complex **2** remains intact up to the melting point at 161–163 °C. This value is in the range of melting temperatures for TRIMEB inclusion complexes and differs from the melting points of known crystalline forms of TRIMEB itself (148 °C, 157 °C)[23] measured by DSC. Complex decomposition is reflected in the mass loss (e) following complex fusion.

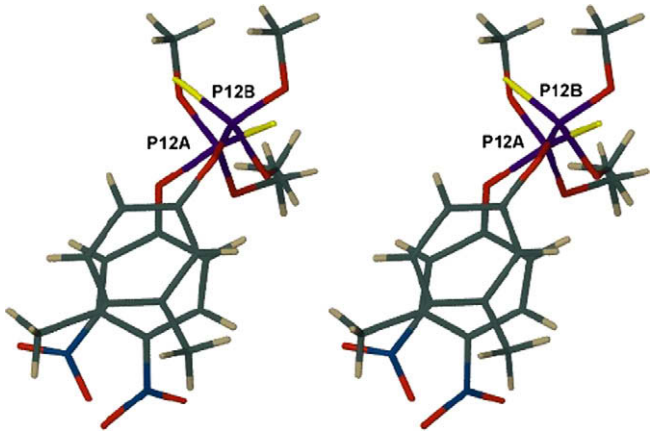

Figure 7. Stereoview illustrating the disorder model for the fenitrothion molecule in complex **2**.

4. Conclusion

X-ray structural investigation of the novel dimeric complex $(TRIMEA)_2$·fenitrothion **1** shows that both the aromatic and the phosphate ester moieties of the fenitrothion molecule have the ability to enter the cavity of the TRIMEA molecule. However, significant strain is induced by inclusion of the aromatic residue, as evidenced by the accompanying distortion of the host molecule which accommodates it. In the case of the larger macrocyclic host, a monomeric complex TRIMEB·fenitrothion **2** results and again the phosphate ester moiety is fully included in the host cavity. These conclusions, drawn from solid-state studies, are pertinent to ongoing research on the chemical stabilization of fenitrothion by CD

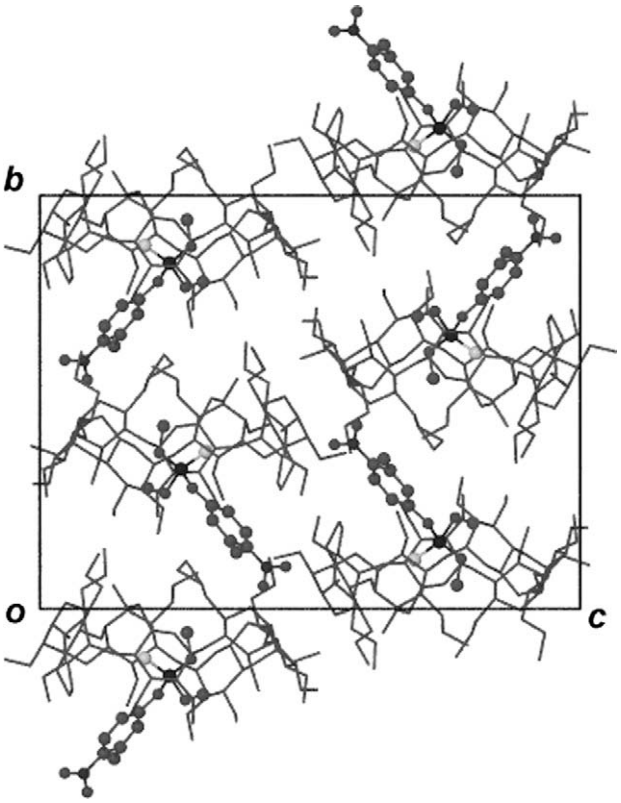

Figure 8. Crystal packing in complex **2** viewed down [1 0 0].

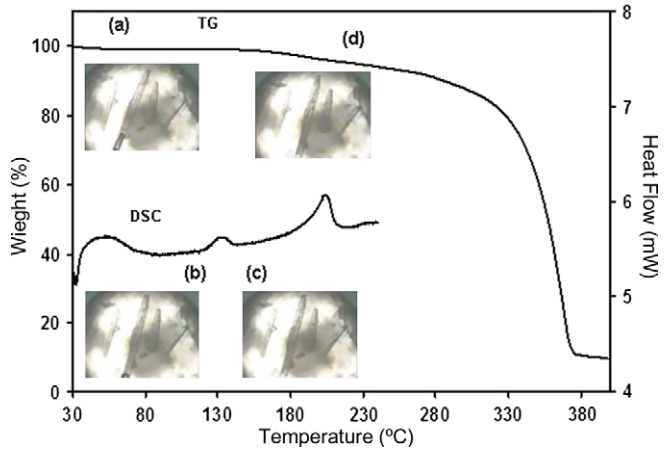

Figure 9. TGA, DSC and HSM data for complex **1**. HSM images were captured at 45 (a), 130 (b), 150 (c) and 200 °C (d). The axis on the left refers to the TGA data while that on the right refers to the DSC data.

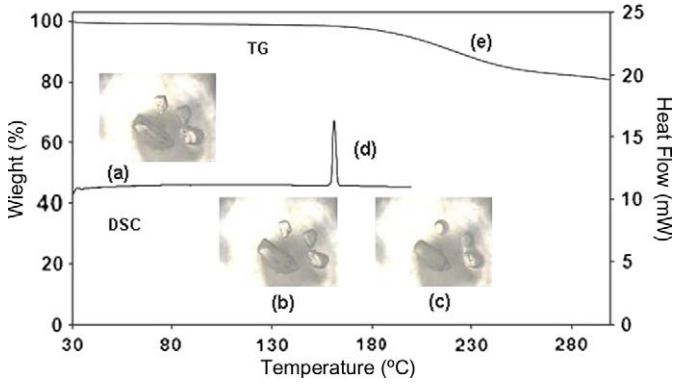

Figure 10. TGA, DSC and HSM data for complex **2**. HSM images were captured at 25 (a), 154 (b) and 163 °C (c). The axis on the left refers to the TGA data while that on the right refers to the DSC data.

inclusion in solution. Our preliminary experiments on the hydrolytic degradation of fenitrothion (involving the sensitive thiophosphate ester moiety) in basic solution indicate a retardation of the reaction rate in the presence of methylated CDs. The observed inhibition could be explained if, in solution, the phosphate ester were similarly included within the host cavity where it would be protected from nucleophilic attack by the hydroxide ion. Further studies aimed at elucidating this aspect are in progress and include NMR spectroscopic investigation of the structures of inclusion complexes between fenitrothion and methylated CDs in solution for comparison with the solid-state results.

Acknowledgements

This material is based upon work supported by the National Research Foundation under Grant number 67381. M.R.C. and D.C. express their thanks to the NRF and the University of Cape Town for financial assistance.

Financial assistance from CONICET, FONCYT, MINCyT-Cordoba (Argentina) and support from the National University of Córdoba are greatly acknowledged. This work was carried out as part of a bilateral cooperation project supported by the NRF (South Africa) and MINCyT (Argentina). NMR is a grateful recipient of a fellowship from YPF Foundation (Argentina).

Supplementary data

Supplementary data associated with this article can be found, in the online version, at doi:10.1016/j.carres.2009.10.023.

References

1. Morillo, E. Applications of Cyclodextrins in Agrochemistry. In *Cyclodextrins and Their Complexes*; Dodziuk, H., Ed.; Wiley-VCH GmBH & Co. KgaA: Weinheim, 2006; pp 459–466.
2. Ishiwata, S.; Mamoru, K. *Chemosphere* **1999**, *39*, 1595–1600.
3. Vico, R. V.; Buján, E. I.; de Rossi, R. H. *J. Phys. Org. Chem.* **2002**, *15*, 858–862.
4. Szente, L.; Magisztrak, H.; Szejtli, J. *Pestic. Sci.* **1990**, *28*, 7–16.
5. Oreste, P.; Borzatta, V.; Delogu, G.; Capparella, E.; De Candia, C.; Gobbi, C.; Di Blasi, G. PCT Int. Appl. WO 2006-EP61724 20060421, 2006.
6. Shibauchi, I. Appl. JP 84-188212 19840910, 1986.
7. Szente, L. *J. Therm. Anal. Calorim.* **1998**, *51*, 957–963.
8. *Cambridge Structural Database and Cambridge Structural Database System, Conquest* Version 1.11, Cambridge Crystallographic Data Centre, University Chemical Laboratory: Cambridge, England, 2009.
9. Greenhalgh, R.; Blackwell, B.; Preston, C.; Murray, W. *J. Agric. Food Chem.* **1983**, *31*, 710–713.
10. Program SAINT, Version 7.60a, Bruker AXS Inc., Madison, WI, USA, 2006.
11. Otwinowski, Z.; Minor, W.. In *Processing of X-ray Diffraction Data in Oscillation Mode in Methods in Enzymology*; Carter, C. W., Sweet, R. M., Eds.; Academic Press: New York, 1996; Vol. 276, pp 307–326.
12. Program SADABS, Version 2.05, University of Göttingen: Germany, 1997.
13. Sheldrick, G. M. In *Direct Methods for Solving Macromolecular Structures*; Fortier, S., Ed.; Kluwer Academic Publishers: Dordrecht, 1998; pp 401–411.
14. Caira, M. R.; Griffith, V. J.; Nassimbeni, L. R.; van Oudtshoorn, B. *J. Inclusion Phenom.* **1995**, *20*, 277–290.
15. Sheldrick, G. M. *Acta Crystallogr., Sect. A* **2008**, *64*, 112–122.
16. Frömming, K-. H.; Szejtli, J.. In *Topics in Inclusion Science—Cyclodextrins in Pharmacy*; Kluwer Academic: Dordrecht, The Netherlands, 1993; Vol. 5.
17. Tsuji, K.; Horide, F.; Minobe, M.; Sasaki, M.; Masao, S.; Shiraga, N.; Hiroaki, O. *Nippon Noyaku Gakkaishi* **1980**, *5*, 371–384.
18. Maeda, T.; Kawashima, M.; Tsuji, K. *Nippon Noyaku Gakkaishi* **1983**, *8*, 339–345.
19. (a) Fukuto, T. R.; Hornig, E. O.; Metcalf, R. L. *J. Agric. Food Chem.* **1964**, *12*, 169–171; (b) Miles, J. W.; Mount, D. L.; Staiger, M. A.; Teeters, W. R. *J. Agric. Food Chem.* **1979**, *27*, 421–425.
20. Han, X. M.; Balakrishnan, V. K.; van Loon, G. W.; Buncel, E. *Langmuir* **2006**, *22*, 9009–9017.
21. Caira, M. R.; Mhlongo, W. T.; Li, J. *J. Optoelect. Adv. Mater.* **2008**, *10*, 2255–2260.
22. Caira, M. R.; Nassimbeni, L. R. Phase Transformations in Inclusion Compounds, Kinetics and Thermodynamics of Enclathration. In *Comprehensive Supramolecular Chemistry*; Atwood, J. L., Davies, J. E. D., Macnicol, D. D., Vögtle, F., Eds.; Pergamon, 1996; Vol. 6,.
23. Caira, M. R.; Bourne, S. A.; Mhlongo, W. T.; Dean, P. M. *Chem. Commun.* **2004**, 2216–2217.